

Control Parameter Description of Eukaryotic Chemotaxis

Gabriel Amselem,¹ Matthias Theves,^{1,2} Albert Bae,^{1,3} Carsten Beta,^{1,2} and Eberhard Bodenschatz^{1,3,4}

¹Max Planck Institute for Dynamics and Self-Organization, Am Faßberg 17, Göttingen D-37077, Germany

²Institute of Physics and Astronomy, University of Potsdam, Karl-Liebknecht-Strasse 24/25, Potsdam 14476, Germany

³Laboratory of Atomic and Solid-State Physics, Cornell University, Ithaca, New York 14853, USA

⁴Sibley School for Mechanical Engineering, Cornell University, Ithaca, New York 14853, USA

(Received 12 January 2012; published 5 September 2012)

The chemotaxis of eukaryotic cells depends both on the average concentration of the chemoattractant and on the steepness of its gradient. For the social amoeba *Dictyostelium discoideum*, we test quantitatively the prediction by Ueda and Shibata [Biophys. J. 93, 11 (2007)] that the efficacy of chemotaxis depends on a single control parameter only, namely, the signal-to-noise ratio (SNR), determined by the stochastic fluctuations of (i) the binding of the chemoattractant molecule to the transmembrane receptor and (ii) the intracellular activation of the effector of the signaling cascade. For $\text{SNR} \leq 1$, the theory captures the experimental findings well, while for larger SNR noise sources further downstream in the signaling pathway need to be taken into account.

DOI: 10.1103/PhysRevLett.109.108103

PACS numbers: 87.17.Jj, 87.16.Xa, 87.18.Tt

Chemotaxis, the directed motion of cells in response to a chemical gradient, is essential in biological phenomena such as wound healing [1], cancer cell metastasis [2], or embryogenesis [3]. A model organism for eukaryotic chemotaxis is *Dictyostelium discoideum*, an amoeba with a typical size of 10 μm , which is able to sense gradients of cyclic adenosine monophosphate (cAMP) and to migrate directionally in chemoattractant gradients, where the difference of bound receptors ΔR between the front and the back of the cell is of the order of 100 out of 30 000 occupied receptors [4].

The efficacy of chemotaxis is influenced by two parameters: the average concentration of cAMP (C) and the gradient steepness ($|\nabla C|$). Recently, Fuller *et al.* [5] presented an experimental study of the influence of these two parameters on chemotactic behavior, where the ratio of gradient steepness to average concentration was constant. They computed the mutual information between the input gradient and the cell motility direction and found that for shallow relative gradients and for small average concentrations the loss of information could be attributed to the noise at the receptor level, while for large average concentrations and steeper gradients it was dominated by intracellular signaling. Earlier, Ueda and Shibata [6] chose another approach by calculating the noise at the receptor level as well as the intracellular noise coming from the effector of the second messenger system, downstream of the receptor. They defined the signal-to-noise ratio at the second effector level, SNR_G , and calculated it for *D. discoideum* at the level of the heterotrimeric guanine nucleotide-binding protein (G protein), whose dissociation occurs directly after receptor binding. They compared their theory with the experimental results by Fisher *et al.* [7] and found reasonable agreement at the population level by considering the average chemotactic efficacy of the cell

population as a function of the SNR_G in the middle of the average cell path. A quantitative comparison with the theory requires the measurement of the chemotactic efficacy of single cells to the local SNR_G along their paths through the gradient.

In this Letter, we show that the description of Ueda and Shibata [6] captures the statistics of single-cell chemotaxis quantitatively for values of the $\text{SNR}_G \leq 1$. For $\text{SNR}_G \geq 1$, noise downstream in the signaling pathway needs to be considered. We exposed individual cells to different gradients of chemoattractant and tracked them for 1 h. At each location along each cell's trajectory, we measured the chemotactic velocity and the chemotactic index (CI) and

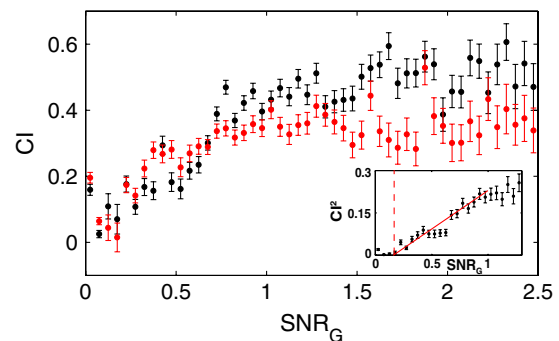


FIG. 1 (color online). CI as a function of the signal-to-noise ratio at the level of the G protein (SNR_G). Red (gray in the printed version) points are for cells in a high average concentration of the chemoattractant cAMP. Black points are for cells in a low average concentration of the chemoattractant cAMP. While for $\text{SNR}_G \leq 1$ all data collapse for all gradients and average concentrations, for $\text{SNR}_G \geq 1$ the observed CI saturates but to values dependent on the average concentration. Inset: squared chemotactic index as a function of the SNR_G for all average concentrations and for $\text{SNR}_G \leq 1$.

calculated the SNR_G . As shown in Fig. 1, for $\text{SNR}_G \lesssim 1$ the measured CI is well captured by the SNR_G while for $\text{SNR}_G \gtrsim 1$ the observed CI saturates to values dependent on the average concentration. Moreover, we found that the SNR_G determines the percentage of motile cells.

Experimental procedures.—As described in detail in [8], *D. discoideum* AX3 cells were grown in HL5 medium and harvested in the exponential growth phase. Then, they were starved for 5 h 30 min in a phosphate buffer and stimulated with cAMP every 6 min during the last five hours of starvation. The cells were loaded into the main channel of the microfluidic gradient device as previously described [4]. The microfluidic gradient device produced stable linear gradients and had the advantage to wash away any cellular signaling molecules. This could be accomplished for shear rates small enough not to cause mechanotaxis [9,10]. Cells were imaged every 40 s using differential interference contrast microscopy and automatically located using a modified version of the algorithm proposed by Kam [11]. Then, they were tracked with an adapted version of the algorithm by Crocker and Grier [12]. For each linear gradient, 50–100 cell tracks were recorded with path durations of 10–30 min (see, e.g., Fig. 2). Immobile cells, defined as cells that moved less than 30 μm in 10 min, were identified and excluded from further processing. At each time step, the cell velocity was estimated using a backward-time difference scheme, and the CI was calculated as the ratio between the cell velocity in the gradient direction v_y and the cell's speed.

Chemotactic sensing.—At 6 h into the development of a *D. discoideum* cell, approximately 80 000 cAMP transmembrane receptors (cAR1) are expressed over the cell membrane [13]. These transmembrane receptors are

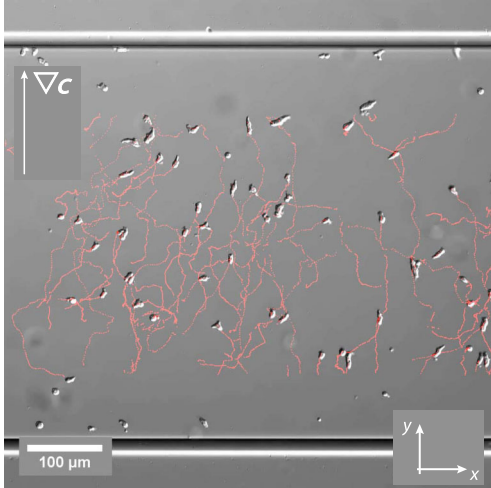
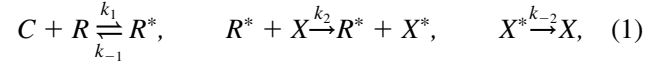


FIG. 2 (color online). Tracks of starved, chemotactic AX3 *D. discoideum* cells in a linear gradient with $c_{\min} = 0$ at the bottom and $c_{\max} = 50$ nM at the top. Cells were tracked for 40 min after the establishment of the gradient ∇c that points upwards in the y direction.

known to stay uniformly distributed with no preference towards the chemotactic gradient [14]. On the binding of cAMP to cAR1, a G protein is activated and splits into two subunits. The $G_{\beta\gamma}$ subunit acts as the main transducer of chemotactic signals [15]. G -protein activation triggers downstream signaling, leading to cellular migration in the gradient direction. Following Ueda and Shibata [6], we consider only these first two events in the chemotactic pathway. We also extend their analysis to arbitrarily steep gradients.

The receptor and second messenger kinetics can be written as [6]



where C is the extracellular cAMP that binds to R , the free receptor cAR1, with a rate k_1 . The unbinding rate is k_{-1} . R^* is the bound cAR1, with $R + R^* = R_{\text{tot}}$. The activation rate of the G protein is k_2 , and its deactivation rate is k_{-2} . X and X^* represent the inactive (respectively activated) G protein ($X + X^* = X_{\text{tot}}$). All these rate constants, except k_{-2} , have been experimentally determined, as have been the total numbers of cAR1 and G proteins [16–19]. The rate constant k_{-2} was estimated to be 1 s^{-1} . We define $K_R = k_{-1}/k_1$ and $K_X = k_{-2}/k_2$. In the following, we assume receptors and G proteins to be immobile along the membrane.

In general, cells are elongated, three dimensional, and migrate at angles to the gradient. As a first approximation, however, we may consider a 1D cell of length L , migrating in the gradient direction (y direction) in a concentration profile $c(y)$. We call $\rho^*(y)$ the local density of bound receptors [$R^* = \int_{-L/2}^{L/2} \rho^*(y) dy$] and $\chi^*(y)$ the local density of activated G proteins [$X^* = \int_{-L/2}^{L/2} \chi^*(y) dy$]. The local density of bound receptors and activated G proteins are following Michaelis-Menten kinetics: $\rho^*(y) = \frac{R_{\text{tot}}}{L} \frac{c(y)}{c(y) + K_R}$, and $\chi^*(y) = \frac{X_{\text{tot}}}{L} \frac{\rho^*(y)}{\rho^*(y) + K_X/L}$. Both reactions are Poisson processes, for which we can define the time constants $\tau_R(y) = [k_1 c(y) + k_{-1}]^{-1}$ and $\tau_X(y) = [k_2 \rho^*(y) L + k_{-2}]^{-1}$. The gains of the two reactions can be written as $g_R(y) = K_R [K_R + c(y)]^{-1}$ and $g_X(y) = K_X [K_X + \rho^*(y) L]^{-1}$. The amplitude of the fluctuations at the receptor level is then given by $\sigma_R^2(y) = g_R(y) \rho^*(y)$, and the amplitude of the noise of the second reaction is [6]

$$\sigma_X^2(y) = g_X(y) X^*(y) + g_X(y)^2 \frac{\tau_R(y)}{\tau_R(y) + \tau_X(y)} \sigma_R(y)^2 \left[\frac{X^*(y)}{R^*(y)} \right]^2. \quad (2)$$

The difference ΔX^* in the number of activated G proteins between the front and back halves of the cell is given by $\Delta X^*(y) = \int_{y+L/2}^y \chi^*(y') dy' - \int_{y-L/2}^y \chi^*(y') dy'$. If we assume local dynamics of the chemical processes, the signal-to-noise ratio is

TABLE I. Parameters used to estimate the SNR. All parameters can be inferred from experiments [16–19], except for k_{-2} . The deactivation and activation rates of the G protein k_{-2} and k_2 are related through $K_X = k_{-2}/k_2$, and K_X was calculated from experimental measures in Ref. [6]. k_{-2} was estimated to 1.0 s^{-1} , and then $k_2 = k_{-2}/K_X$.

Parameter		Value
R_{tot}	Number of cAMP receptors	80 000 molecules/cell
k_1	Association rate of cAMP	$5.6 \text{ s}^{-1} \mu\text{M}^{-1}$
k_{-1}	Dissociation rate of cAMP	1 s^{-1}
X_{tot}	Number of G proteins	200 000 molecules/cell
k_2	Activation rate of the G protein	$1/4210$
		$\text{s}^{-1}(\text{molecules/cell})^{-1}$
k_{-2}	Deactivation rate of the G protein	1.0 s^{-1}

$$\text{SNR}_G(y) = \frac{|\Delta X^*(y)|}{\sigma_{\Delta X^*(y)}} = \frac{|\int_{y-L/2}^{y+L/2} \chi^*(y') dy' - \int_{y-L/2}^y \chi^*(y') dy'|}{\int_{y-L/2}^{y+L/2} \sigma_X^2(y') dy'}. \quad (3)$$

Results.—With Eq. (3), we calculate the $\text{SNR}_G(y)$ along the cells' trajectories with the biological parameters given by Ueda and Shibata [6] (see Table I). The chemotactic index was recorded at each time step. The data were first binned according to the value of the SNR_G and at each value of the SNR_G were subsequently divided into two regions, depending on the average concentration of cAMP at the location of the cell. The evolution of the average CI, as a function of the SNR_G , can be seen in Fig. 1. For each bin of the SNR_G , the black point shows the average CI of cells with an average concentration of cAMP less than the median concentration of cAMP surrounding the cells in this bin. The red point (gray in the printed version) shows the average CI of cells experiencing a concentration greater than the median. The agreement between the two curves for $\text{SNR}_G \lesssim 1$ shows that the efficacy of chemotaxis is controlled by the SNR_G in this region. The inset in Fig. 1 shows CI^2 as a function of SNR_G . The linear behavior may be indicative of a forward bifurcation with SNR_G as a control parameter. The CI saturates for $\text{SNR}_G \gtrsim 1$ to a value depending on the average concentration surrounding the cells. This points to the presence of more noise downstream of the signaling cascade. In particular, the higher the average concentration a cell experiences, the more reactions downstream of the cascade make a significant contribution to the total intracellular noise [6,20]. At a given value of the SNR_G , cells in a high average concentration of cAMP therefore have a smaller CI than cells in a low average concentration of cAMP; see Fig. 1. The same data binned according to the SNR_G and the gradient are shown in the Supplemental Material [21]. For further reference, we show in Fig. 3 a level plot of the SNR_G as a function of the midpoint concentration and the ratio $\rho = \Delta C/C$, where C is the average and $\Delta C = L|\nabla C|$ is the difference of cAMP concentration across a cell.

We also show the range of our measurements. Note that $0 \leq \rho \leq 2$, as the average concentration $C = C_{\text{low}} + (L/2)|\nabla C|$, where C_{low} is the concentration at the cell membrane at the low side of the gradient.

In studies of chemotaxis, it is common to discard cells that move a distance less than a threshold distance and to consider these cells as immobile [5,22]. The analysis of chemotaxis is then performed only on the motile cells. We find that the SNR_G determines the fraction of motile cells, with more cells motile at higher SNR_G . For each experimental condition, the value of the SNR_G was estimated in the middle of the microfluidic device, and immobile cells were defined as cells whose displacement is smaller than a threshold distance of $30 \mu\text{m}$ in 10 min. We checked that our results were qualitatively unchanged when the threshold distance was varied. As shown in Fig. 4, the fraction of mobile cells in a channel goes up as the SNR_G in the middle of the channel increases.

Conclusion.—We found that the fraction of mobile cells in a population increased with the SNR_G and that the SNR_G parametrizes well the chemotactic behavior of

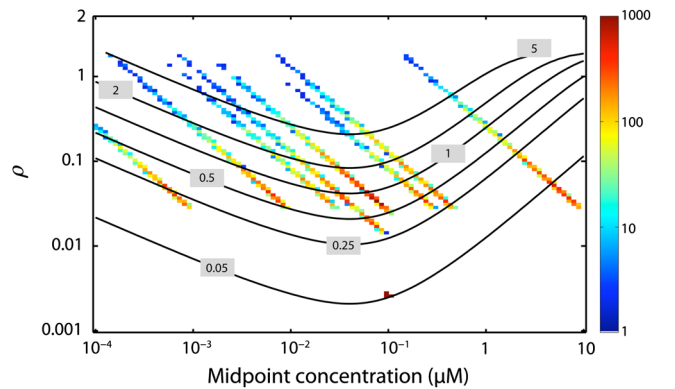


FIG. 3 (color online). Black lines: contour plot of the value of the SNR_G as a function of the midpoint concentration and the ratio $\rho = \Delta C/C$. The SNR_G was calculated using Eq. (3). The labels mark the SNR_G value of each contour. We binned our data according to gradient and midpoint concentration and show in color (gray scale in the printed version) the number of measurements in each bin.

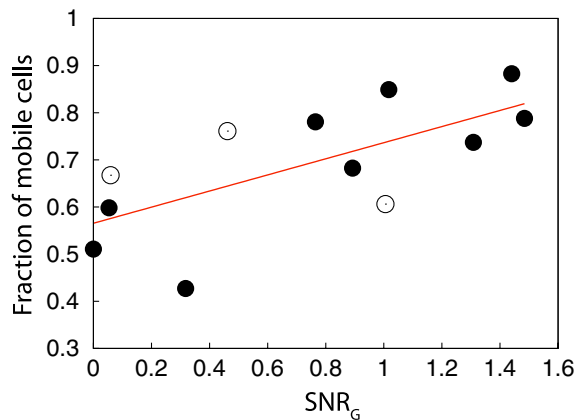


FIG. 4 (color online). Fraction of mobile cells in a microfluidic device as a function of the SNR_G in the middle of the device. The red line is a linear fit to the data. Filled black circles: data for linear concentration gradients from 0 to a concentration c_{\max} . Empty black circles: data for linear concentration gradients from $c_{\min} \neq 0$ to c_{\max} (see Supplemental Material [21] for values of c_{\min} and c_{\max}).

Dictyostelium cells for $\text{SNR}_G \leq 1$, where the chemotactic efficacy increases with larger SNR_G , and the SNR_G appears to be the single order parameter. At $\text{SNR}_G \geq 1$, the cells' chemotactic precision saturates and is not limited by the signal-to-noise ratio at the level of the G protein but by noise sources related to events further downstream in the regulatory processes. As shown in the inset of Fig. 1, our data also suggest a minimal value of the SNR_G necessary for chemotaxis.

Previous work by Endres and Wingreen [23] and by Van Haastert and Postma [24] showed that the SNR at the receptor level can fully characterize the chemotactic behavior of *D. discoideum* in gradients with low midpoint concentrations [25]. This is in agreement with our findings. Note that the noise at the second messenger level is a combination of the stochastic fluctuations at the level of the receptor and at the level of the second messenger. These two contributions were termed extrinsic and intrinsic noise, respectively, in Ref. [6]. As mentioned in Ref. [6], the noise at the receptor level dominates at low midpoint concentrations, while the intracellular noise dominates at high midpoint concentrations. This interplay between the two noise contributions and their relative importance as a function of the midpoint concentration was the main conclusion of Fuller *et al.* [5], who came to this result using an information-theoretic framework to characterize chemotactic cell motion.

In recent years, the development of microfluidics and the increasing power of personal computers led to an increase in the precision and amount of chemotaxis data that could be taken [4,5,22]. At the same time, several models of directional sensing have been developed. One approach taken to discriminate between them has been to compare their results as a function of the signal-to-noise ratio at the

receptor level [26,27]. We suggest that the different models of directional sensing should rather be evaluated as a function of their response to the SNR_G . Moreover, it is likely that the SNR at the level of the second messenger is also the quantity determining the chemotactic efficiency of other eukaryotic cells. Recently, an attempt to explain the chemotactic prowess of neutrophil-differentiated HL60 cells as a function of the signal-to-noise ratio at the receptor level was reported by Herzmark *et al.* [22]. Yet, the data of Herzmark *et al.* showed that no quantitative relationship existed between the SNR at the receptor level and the chemotactic prowess of the cells. We suggest that the SNR at the level of the second messenger could be the quantity that allows a quantitative explanation of the data presented in Ref. [22]. However, for neutrophil-differentiated HL60 cells, experimental data on the number of second messengers as well as the reaction rates of the activation or deactivation of the second messenger are still missing. With these data at hand, it will be possible to test how we can extend the analysis of the SNR_G to other eukaryotic cells.

-
- [1] T.J. Shaw and P. Martin, *J. Cell Sci.* **122**, 3209 (2009).
 - [2] J. Condeelis, R.H. Singer, and J.E. Segall, *Annu. Rev. Cell Dev. Biol.* **21**, 695 (2005).
 - [3] P. Martin and S.M. Parkhurst, *Development (Cambridge, U.K.)* **131**, 3021 (2004).
 - [4] L. Song, S.M. Nadkarni, H.U. Bödeker, C. Beta, A.J. Bae, C. Franck, W.J. Rappel, W.F. Loomis, and E. Bodenschatz, *Eur. J. Cell Biol.* **85**, 981 (2006).
 - [5] D. Fuller, W. Chen, M. Adler, A. Groisman, H. Levine, W.J. Rappel, and W.F. Loomis, *Proc. Natl. Acad. Sci. U.S.A.* **107**, 9656 (2010).
 - [6] M. Ueda and T. Shibata, *Biophys. J.* **93**, 11 (2007).
 - [7] P.R. Fisher, R. Merkl, and G. Gerisch, *J. Cell Biol.* **108**, 973 (1989).
 - [8] M. Theves, Diplomarbeit, Universität Göttingen and Max-Planck Institut für Dynamik und Selbstorganisation, 2009.
 - [9] C. Beta, T. Fröhlich, H.U. Bödeker, and E. Bodenschatz, *Lab Chip* **8**, 1087 (2008).
 - [10] C. Beta and E. Bodenschatz, *Eur. J. Cell Biol.* **90**, 811 (2011).
 - [11] Z. Kam, *Bioimaging* **6**, 166 (1998).
 - [12] J. Crocker and D. Grier, *J. Colloid Interface Sci.* **179**, 298 (1996).
 - [13] C.A. Parent and P.N. Devreotes, *Science* **284**, 765 (1999).
 - [14] Z. Xiao, N. Zhang, D.B. Murphy, and P.N. Devreotes, *J. Cell Biol.* **139**, 365 (1997).
 - [15] L. Stephens, L. Milne, and P. Hawkins, *Curr. Biol.* **18**, R485 (2008).
 - [16] C. Janetopoulos, T. Jin, and P.N. Devreotes, *Science* **291**, 2408 (2001).
 - [17] M. Ueda, Y. Sako, T. Tanaka, P.N. Devreotes, and T. Yanagida, *Science* **294**, 864 (2001).

- [18] T. Jin, N. Zhang, Y. Long, C.A. Parent, and P.N. Devreotes, *Science* **287**, 1034 (2000).
- [19] P.M. Janssens and P.J.M. Van Haastert, *Microbiol. Rev.* **51**, 396 (1987) [<http://mibr.asm.org/content/51/4/396.full.pdf+html>].
- [20] T. Shibata and K. Fujimoto, *Proc. Natl. Acad. Sci. U.S.A.* **102**, 331 (2005).
- [21] See Supplemental Material at <http://link.aps.org/supplemental/10.1103/PhysRevLett.109.108103> for values of c_{\min} and c_{\max} used in our experiments, comparison of data sets from the literature plotted as a function of the SNR_G , a simple model estimating the CI, and data binning according to the SNR_G and the gradient.
- [22] P. Herzmark, K. Campbell, F. Wang, K. Wong, H. El-Samad, A. Groisman, and H.R. Bourne, *Proc. Natl. Acad. Sci. U.S.A.* **104**, 13 349 (2007).
- [23] R.G. Endres and N.S. Wingreen, *Proc. Natl. Acad. Sci. U.S.A.* **105**, 15 749 (2008).
- [24] P.J. Van Haastert and M. Postma, *Biophys. J.* **93**, 1787 (2007).
- [25] In [24], a constant intracellular noise was assumed in addition to the noise at the receptor level. This constant intracellular noise is in agreement with the data shown in [24] because the concentration profiles used have a low midpoint concentration. At higher midpoint concentrations, the dependence of the intracellular noise on the average concentration of the chemoattractant becomes crucial.
- [26] W. J. Rappel and H. Levine, *Phys. Rev. Lett.* **100**, 228101 (2008).
- [27] W. J. Rappel and H. Levine, *Proc. Natl. Acad. Sci. U.S.A.* **105**, 19 270 (2008).